JACS
JOURNAL OF THE AMERICAN CHEMICAL SOCIETY

COMMUNICATION

pubs.acs.org/JACS

Siloxane-Terminated Solubilizing Side Chains: Bringing Conjugated Polymer Backbones Closer and Boosting Hole Mobilities in Thin-Film Transistors

Jianguo Mei,[†,⊥,§] Do Hwan Kim,[†,⊥] Alexander L. Ayzner,[†,‡] Michael F. Toney,[‡] and Zhenan Bao*[,†]

[†]Department of Chemical Engineering, Stanford University, Stanford, California 94305-5025, United States

[‡]SLAC National Accelerator Laboratory, Stanford Synchrotron Radiation Lightsource, Menlo Park, California 94025, United States

Supporting Information

ABSTRACT: We introduce a novel siloxane-terminated solubilizing group and demonstrate its effectiveness as a side chain in an isoindigo-based conjugated polymer. An average hole mobility of 2.00 $cm^2 V^{-1} s^{-1}$ (with a maximum mobility of 2.48 $cm^2 V^{-1} s^{-1}$), was obtained from solution-processed thin-film transistors, one of the highest mobilities reported to date. In contrast, the reference polymer with a branched alkyl side chain gave an average hole mobility of 0.30 $cm^2 V^{-1} s^{-1}$ and a maximum mobility of 0.57 $cm^2 V^{-1} s^{-1}$. This is largely explained by the polymer packing: our new polymer exhibited a $\pi-\pi$ stacking distance of 3.58 Å, while the reference polymer showed a distance of 3.76 Å.

Solution processability is one of the most distinctive features that set organic semiconducting materials apart from their inorganic counterparts such as silicon-based semiconductors. This property makes conjugated polymers attractive for applications such as low-cost solar cells and field-effect transistors (FETs), owing to their compatibility with widely used fast printing techniques. Solubility of conjugated polymers in common organic solvents (e.g., chloroform, toluene, and chlorobenzene) typically results from the attachment of flexible aliphatic chains as solubilizing groups onto conjugated moieties. The selection of solubilizing groups is an art of balance, as they affect molecular packing, thin-film morphology, and hence material performance in devices.[1] Compared to the vast library of conjugated building blocks,[2] the choice of solubilizing groups is unfortunately limited. Branched alkyl chains such as 2-ethylhexyl, 2-hexyldecyl, and 2-octyldodecyl groups and linear alkyl chains such as hexyl, octyl, and dodecyl groups represent the majority in the family of solubilizing groups. However, the branching point of these branched alkyl chains is close to the conjugated backbone and will likely disrupt the intermolecular $\pi-\pi$ interactions between conjugated backbones. Surprisingly, little attention has so far been given to designing new solubilizing groups for conjugated polymers, in stark contrast to the tremendous efforts made in search for new conjugated building blocks.[1a,3]

Herein, we depart from the conventional approach and focus on the design of solubilizing groups through introducing a novel hybrid solubilizing chain. Using this new side chain, we show that the thin-film field-effect mobility in a conjugated polymer film can be significantly enhanced via a combination of a smaller π-stacking distance, mixed crystallographic orientation (texture), and a larger crystalline coherence length, relative to the control polymer with a common branched aliphatic side chain.

The design features a block of linear alkyl chain and a flexible 1,1,1,3,5,5,5-heptamethyltrisiloxane terminal unit. The Si−O bond length is about 1.64 Å, which is significantly longer than C−C bond length of 1.53 Å, and the Si−O−Si bond angle of 143° is also significantly larger than the usual tetrahedral angle (~110°).[4] By choosing siloxane block as part of the solubilizing chain, we expect to bring great solubility to the resulting conjugated polymers. On the other hand, moving the branched site away from conjugated backbones potentially allows the backbones to come closer and facilitates charge transfer. The siloxane group can also function as a potential cross-linking site if desired. The linear alkyl chain serves as a spacer to fine-tune solubility and control the distance between the conjugated building blocks and the very bulky siloxane group. To test our design concept, we chose isoindigo-based conjugated polymers due to the easy and efficient functionalization of the isoindigo core, as well as their excellent performance in air-stable FETs as demonstrated by Pei et al.[3g]

Synthesis of the reference polymer (**PII2T-Ref**) was based on a reported method,[3g] except that a microwave reactor was used in the polymerization step. The polymerization condition is provided in detail in the Supporting Information. Synthesis of the target polymer (**PII2T-Si**) is shown in Scheme 1. Starting with 2,6-dibromoisoindigo, an alkene-terminated linear alkyl chain was attached to the isoindigo core via base-promoted N-alkylation.[5] Hydrosilylation of the terminal alkene with 1,1,1,3,5,5,5-heptamethyltrisiloxane was successfully achieved in the presence of commercially available Karstedt catalyst, yielding highly soluble isoindigo monomer with siloxane-terminated solubilizing chains.[6] **PII2T-Si** was synthesized under microwave conditions in the same manner as **PII2T-Ref**. Both polymers were purified by precipitation into acetone followed by Soxhlet extraction using acetone, hexane, and chloroform.

As shown in Table 1, high number-average molecular weights (>130 kDa, DP ≈ 130) from gel permeation chromatography using polystyrene as the standard in THF were observed for both **PII2T-Ref** and **PII2T-Si**, with polydispersity of 5.5 and 3.3, respectively. The observed molecular weights as well as the

Received: October 3, 2011
Published: November 28, 2011

polydispersities might be overestimated due to the potential formation of aggregates in THF; nevertheless, they indicate that **PII2T-Ref** and **PII2T-Si** are high polymers. Both polymers were thermally stable over 390 °C as determined by thermogravimetric analysis. No noticeable phase transitions were observed by differential scanning calorimetry in the range of 0−300 °C in both cases.

Absorption profiles of **PII2T-Ref** and **PII2T-Si** in dilute chloroform solutions and in thin films are displayed in Figure 1. In solution, the absorption of **PII2T-Ref** peaks at 706 nm and has an additional higher energy peak at 644 nm. In comparison, **PII2T-Si** shows the absorption maximum at 728 nm and its shoulder at 662 nm. The red-shift (∼25 nm) in solution absorbance onset from **PII2T-Ref** to **PII2T-Si** possibly results from different backbone conformations. Due to the interaction among the neighboring branched octyldodecyl chains, **PII2T-Ref** is likely to adapt a more twisted backbone. In contrast, **PII2T-Si** more likely exhibits a more planar backbone, since steric repulsion between side chains is minimized. In the solid state, the absorption onset of **PII2T-Ref** shows a noticeable red-shift (∼10 nm) relative to the solution spectrum, which is a common observation with most conjugated polymers. However, the absorption onset of **PII2T-Si** in the film undergoes a non-trivial shift to a *shorter* wavelength (∼16 nm) relative to solution. Further experiments are currently underway to reveal the different behaviors between **PII2T-Ref** and **PII2T-Si**.

Scheme 1. Synthetic route to PII2T-Si[a]

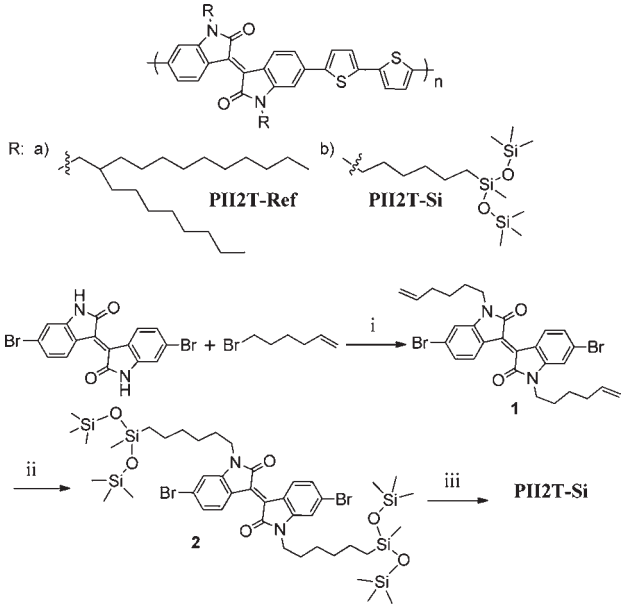

[a] Reagents and conditions: (i) K_2CO_3, DMF, 100 °C, 75%; (ii) Karstedt catalyst, 1,1,1,3,5,5,5-heptamethyltrisiloxane, toluene, 50 °C, 40%; (iii) 5,5′-bis(trimethylstannyl)-2,2′-bithiophene, $Pd_2(dba)_3$, P(*o*-tyl)$_3$, toluene, μW, 91%.

Photoelectron spectroscopy (PES) was used to measure the HOMO energy levels of both polymers.[7] HOMO levels from PES are −5.38 and −5.20 eV for **PII2T-Ref** and **PII2T-Si**, respectively. Using their optical band gaps, we calculated their LUMO values to be approximately −3.77 and −3. 58 eV, respectively. The deeper HOMO level of **PII2T-Ref** may be again due to more severe backbone twisting and their different interchain interactions.

To probe how our side-chain engineering affects charge transport over macroscopic dimensions, we fabricated bottom-gate/top-contact organic FETs (OFETs). Au source/drain electrodes (W = 1000 μm, L = 50 μm) were used to measure the electrical performances of **PII2T-Ref**- and **PII2T-Si**-based devices, and the average field-effect mobilites were calculated from the transfer characteristics of more than 10 devices in the saturation region (V_{DS} = −100 V). The SiO_2 dielectric surface (300 nm) of a heavily n-doped silicon wafer was modified with a dense crystalline octadecyltrimethoxysilane (OTMS) self-assembled monolayer to enhance the electrical performance using a procedure we reported previously.[8] A layer of **PII2T-Ref** and **PII2T-Si** was deposited on top of the OTMS-treated substrate by spin-coating a polymer solution in chlorof orm (4 mg/mL) at 1000 rpm for 60 s. The films thickness was ∼75−83 nm. Figure 2 displays the typical output (I_{DS}−V_{DS}) at different gate voltages (V_{GS}) and transfer (I_{DS}−V_{GS}) characteristics of OFETs based on **PII2T-Ref** and **PII2T-Si** thin films annealed at 170 °C under nitrogen for 1 h. For **PII2T-Ref**, the as-cast films exhibited a low charge carrier mobility of 0.08 $cm^2\ V^{-1}\ s^{-1}$ ($I_{on}/I_{off} > 10^5$). However, after 1 h of annealing at 170 °C, the mobility increased to 0.33 ± 0.14 $cm^2\ V^{-1}\ s^{-1}$, maintaining an on/off current ratio of 10^5. The obtained results are comparable to the literature reported values as shown in Table 2.

In contrast, the mobility of the as-cast **PII2T-Si** film was measured to be 0.45 $cm^2\ V^{-1}\ s^{-1}$ ($I_{on}/I_{off} > 10^6$) (Table 2).

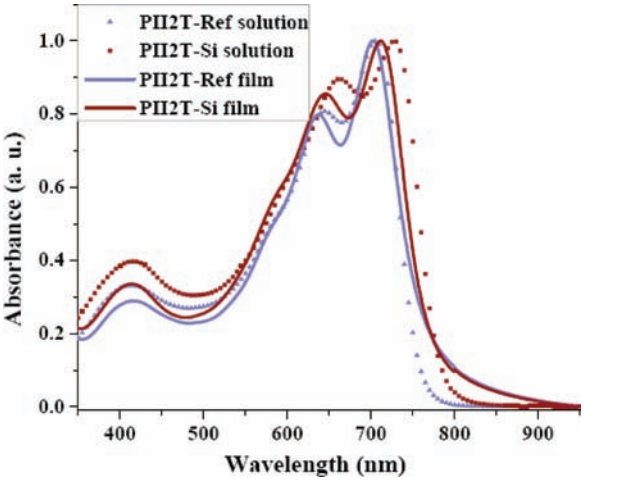

Figure 1. Normalized absorption spectra in dilute solution (chloroform) and thin films (cast from chloroform) of **PII2T-Ref** (blue) and **PII2T-Si** (red).

Table 1. Properties of PII2T-Ref and PII2T-Si

	M_n (kDa)	M_w (kDa)	PDI	T_d (°C)	λ_{max} (nm), sol[a]	λ_{max} (nm), film	HOMO (eV)[b]	band gap (eV)[c]
PII2T-Ref	135	742	5.5	418	706, 644	702, 638	5.38	1.62
PII2T-Si	138	454	3.3	396	728, 662	712, 646	5.20	1.61

[a] In dilute chloroform. [b] Determined by UV-PES. [c] Estimated from thin-film absorption onset.

dx.doi.org/10.1021/ja209328m |*J. Am. Chem. Soc.* 2011, 133, 20130–20133

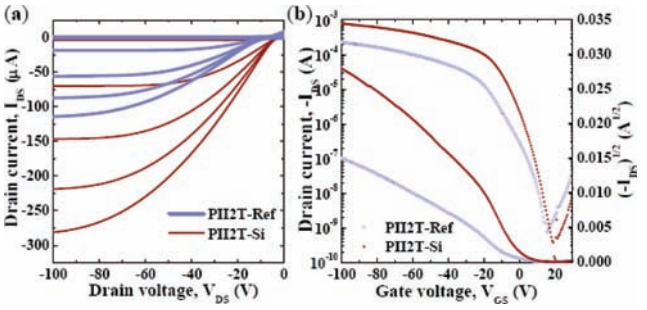

Figure 2. (a) Output and (b) transfer characteristics ($V_{DS} = -100$ V) for **PII2T-Ref**- and **PII2T-Si**-based OFET devices annealed at 170 °C. In the output plots, the gate voltage varies from 0 to −100 V (channel width, 1000 μm; channel length, 50 μm). The hole mobility of 2.45 $cm^2 V^{-1} s^{-1}$ in the saturation regime was calculated from the slopes obtained by linear fitting of $(I_{DS})^{1/2}$ vs V_{GS} in the V_{GS} range from −9 to −16 V.

Table 2. OFET Properties of As-Spun and Annealed PII2T-Ref and PII2T-Si

	as-spun			annealed at 170 °C[a]		
	μ ($cm^2 V^{-1} s^{-1}$)	I_{on}/I_{off}	V_{th}	μ ($cm^2 V^{-1} s^{-1}$)	I_{on}/I_{off}	V_{th}
PII2T-Ref	0.08 (±0.01)	$>10^5$	1	0.33 (±0.13) [0.57][b]	$>10^5$	−2
PII2T-Ref[c]	0.1−0.2	$\sim10^6$	n/a	0.42 [0.79][b]	$\sim10^7$	n/a
PII2T-Si	0.45 (±0.03)	$>10^5$	5	2.00 (±0.49) [2.48][b]	$>10^6$	3

[a] Measured under nitrogen. [b] Maximum mobilities are shown in brackets. The **PII2T-Ref** and **PII2T-Si** OFET mobilities are averages of 10 devices (L = 50 μm and W = 1000 μm), and the error bars denote standard deviations. [c] Data from ref 3g.

When **PII2T-Si** film was annealed at 150 °C, the mobility increased to 1.78 ± 0.35 $cm^2 V^{-1} s^{-1}$ and rose further to 2.0 ± 0.49 $cm^2 V^{-1} s^{-1}$ upon annealing at 170 °C (Figure S1). These characteristics are similar irrespective of measurement condition (in air and under N_2) (see Figure S2). The maximum mobility of the **PII2T-Si**-based devices was determined to be as high as 2.48 $cm^2 V^{-1} s^{-1}$. Even though the annealing temperature is high for low-cost polyester substrates, this approach can be applied to other polymers which may have higher glass transition temperatures. Further process interface optimization may also lower the annealing temperature. We should also mention that both **PII2T-Ref** and **PII2T-Si** devices were stable against atmospheric oxygen, with only slight degradation in mobility when the films were stored under ambient conditions for 30 days (RH = 40−45%) (Figures S3 and S4).

The unusually high hole mobility for **PII2T-Si**-based OFET is likely due to the stronger intermolecular interactions of this polymer in the solid state relative to **PII2T-Ref** films. In general, donor−acceptor-type polymers have a tendency to form interchain aggregates by virtue of strong $\pi-\pi$ stacking, which leads to efficient charge transport in devices.[9] To investigate the correlation between molecular packing and transistor performance, we performed grazing incidence X-ray diffraction (GIXD) experiments on thin-film samples cast onto OTMS-covered Si substrates. Figure 3 shows 2-D GIXD images of **PII2T-Ref** and **PII2T-Si** films, and the relevant crystallographic parameters are summarized in Table 3.

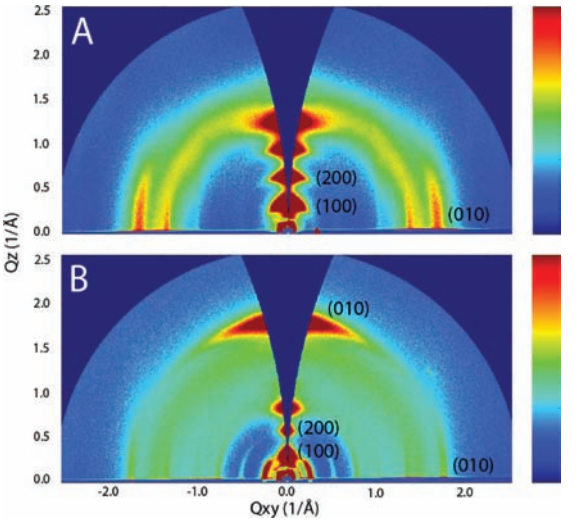

Figure 3. GIXD images of **PII2T-Ref** (A) and **PII2T-Si** (B) annealed at 130 °C **PII2T-Ref** displays lamellar packing common to many conjugated polymer films, with the π-stacking Bragg planes parallel to the substrate plane. In contrast, **PII2T-Si** crystallites contain two kinds of textures, where the π-stacking planes are both normal and parallel to the substrate.

Table 3. Relevant Crystallographic Parameters for the Two Polymer Films

	$\pi-\pi$ Q_{xy} ($Å^{-1}$)	$\pi-\pi$ spacing (Å)	in-plane fwhm ($Å^{-1}$)	in-plane coherence length (Å)	a^* ($Å^{-1}$)	lamellar spacing (Å)
PII2T-Ref	1.675	3.75	0.116	79.6	0.310	20.3
PII2T-Si	1.754	3.58	0.082	137.9	0.276	22.8

The **PII2T-Ref** film displays lamellar texture as judged by the presence of the (h00) Bragg peaks (corresponding to the reciprocal lattice vector a*) falling on the out-of-plane Q_z axis, which is common to many conjugated polymers. The reflection corresponding to π-stacking planes is strongest along the in-plane Q_{xy} axis, showing that the orientation of these planes is largely perpendicular to the substrate (the π-stacking is in-plane).

Figure 3B shows that the texture of the **PII2T-Si** film is quite different from that of **PII2T-Ref**. Specifically, **PII2T-Si** crystallites appear to have dual texture: the (h00) Bragg peak shows both out-of-plane and in-plane orientations. This is most apparent with the π-stacking peak (Q = 1.75 $Å^{-1}$). Interestingly, the π-stacking distance for **PII2T-Si** (3.58 Å) is smaller than that of **PII2T-Ref** (3.75 Å) by 0.17 Å. Moreover, according to Scherrer analysis, the crystalline coherence length of the *in-plane* π-stacking Bragg reflection is larger for **PII2T-Si** (138 Å) relative to its alkyl analogue (80 Å). The coherence length is related to both the total number of scattering lattice plains in a given crystallite and the degree of crystalline disorder.[10]

It is well established that charge carrier mobilities in conjugated polymer films are very sensitive functions of the intermolecular overlap integral.[11] Therefore, all else being equal, crystallites with smaller $\pi-\pi$ distances are expected to yield higher mobilities. This helps explain why the FET mobility is higher for **PII2T-Si** compared to **PII2T-Ref**. In addition, since all spin-coated semicrystalline conjugated polymer films are

dx.doi.org/10.1021/ja209328m |J. Am. Chem. Soc. 2011, 133, 20130–20133

polycrystalline, charges must inevitably hop across grain boundaries as they traverse the macroscopic conduction channel length. Therefore, a larger crystalline coherence length is beneficial for lowering the density of parasitic grain boundaries.

Finally, the dramatic texture difference could also contribute to the mobility differences that we observe. Transport in the transistor configuration occurs primarily in-plane, and in particular in conjugated polymers, holes and electrons move along the π-stacking direction. However, it is conceivable that when a carrier encounters a grain boundary with unfavorable mutual orientation between the grains, the ability to move around such a boundary in the direction normal to the substrate plane could be beneficial for charge transport. In this respect, it is again expected that charges in a **PII2T-Si** film could utilize such 3-D conduction channels more effectively relative to **PII2T-Ref** due to the presence of both parallel and perpendicular orientations of π-stacking planes. Similar texture has been reported for other high-mobility polymers.[12]

In summary, we demonstrated that the use of siloxane-terminated solubilizing groups can bring sufficient solubility to conjugated polymers for solution processing. Even more intriguing is the fact that we found an FET hole mobility up to 2.48 $cm^2 V^{-1} s^{-1}$ for **PII2T-Si**, in comparison to 0.57 $cm^2 V^{-1} s^{-1}$ for **PII2T-Ref**. Conceivably, this strategy of using siloxane-terminated solubilizing groups can be extended to other conjugated systems, such as diketopyrrolopyrrole-based conjugated polymers.

■ ASSOCIATED CONTENT

Supporting Information. Complete ref 7, synthetic details, materials characterizations, and device fabrication procedure. This material is available free of charge via the Internet at http://pubs.acs.org

■ AUTHOR INFORMATION

Corresponding Author
zbao@stanford.edu

Present Addresses
[§]DuPont R&D and Management Co. Ltd., Shanghai, China

Author Contributions
[⊥]These authors contributed equally.

■ ACKNOWLEDGMENT

This work was partially supported by the Center for Advanced Molecular Photovoltaics, award no. KUS-C1-015-21, made by King Abdullah University of Science and Technology. We also acknowledge support from the Global Climate and Energy Program at Stanford. GIXD measurements were carried out at the Stanford Synchrotron Radiation Laboratory, a national user facility operated by Stanford University on behalf of the U.S. Department of Energy, Office of Basic Energy Sciences. J.M. thanks the Camille and Henry Dreyfus Postdoctoral Program in Environmental Chemistry for a postdoctoral fellowship.

■ REFERENCES

(1) (a) Tsao, H. N.; Cho, D. M.; Park, I.; Hansen, M. R.; Mavrinskiy, A.; Yoon, D. Y.; Graf, R.; Pisula, W.; Spiess, H. W.; Müllen, K. *J. Am. Chem. Soc.* **2011**, *133*, 2605. (b) Piliego, C.; Holcombe, T. W.; Douglas, J. D.; Woo, C. H.; Beaujuge, P. M.; Fréchet, J. M. J. *J. Am. Chem. Soc.* **2010**, *132*, 7595.

(2) (a) Cheng, Y.-J.; Yang, S.-H.; Hsu, C.-S. *Chem. Rev.* **2009**, *109*, 5868. (b) Carsten, B.; He, F.; Son, H. J.; Xu, T.; Yu, L. *Chem. Rev.* **2011**, *111*, 1493. (c) Grimsdale, A. C.; Leok Chan, K.; Martin, R. E.; Jokisz, P. G.; Holmes, A. B. *Chem. Rev.* **2009**, *109*, 897.

(3) (a) He, F.; Wang, W.; Chen, W.; Xu, T.; Darling, S. B.; Strzalka, J.; Liu, Y.; Yu, L. *J. Am. Chem. Soc.* **2011**, *133*, 3284. (b) Son, H. J.; Wang, W.; Xu, T.; Liang, Y.; Wu, Y.; Li, G.; Yu, L. *J. Am. Chem. Soc.* **2011**, *133*, 1885. (c) Varotto, A.; Treat, N. D.; Jo, J.; Shuttle, C. G.; Batara, N. A.; Brunetti, F. G.; Seo, J. H.; Chabinyc, M. L.; Hawker, C. J.; Heeger, A. J.; Wudl, F. *Angew. Chem., Int. Ed.* **2011**, *50*, 5166. (i) Zhou, H.; Yang, L.; Stuart, A. C.; Price, S. C.; Liu, S.; You, W. *Angew. Chem., Int. Ed.* **2011**, *50*, 2995. (d) Amb, C. M.; Chen, S.; Graham, K. R.; Subbiah, J.; Small, C. E.; So, F.; Reynolds, J. R. *J. Am. Chem. Soc.* **2011**, *133*, 10062. (e) Zhang, W.; Smith, J.; Watkins, S. E.; Gysel, R.; McGehee, M.; Salleo, A.; Kirkpatrick, J.; Ashraf, S.; Anthopoulos, T.; Heeney, M.; McCulloch, I. *J. Am. Chem. Soc.* **2010**, *132*, 11437. (f) Wang, M.; Hu, X.; Liu, P.; Li, W.; Gong, X.; Huang, F.; Cao, Y. *J. Am. Chem. Soc.* **2011**, *133*, 9638. (g) Lei, T.; Cao, Y.; Fan, Y.; Liu, C.-J.; Yuan, S.-C.; Pei, J. *J. Am. Chem. Soc.* **2011**, *133*, 6099. (h) Wang, E.; Ma, Z.; Zhang, Z.; Vandewal, K.; Henriksson, P.; Inganäs, O.; Zhang, F.; Andersson, M. R. *J. Am. Chem. Soc.* **2011**, *133*, 14244.

(4) Mark, J. E. *Acc. Chem. Res.* **2004**, *37*, 946.

(5) Mei, J.; Graham, K. R.; Stalder, R.; Reynolds, J. R. *Org. Lett.* **2010**, *12*, 660.

(6) Dantlgraber, G.; Eremin, A.; Diele, S.; Hauser, A.; Kresse, H.; Pelzl, G.; Tschierske, C. *Angew. Chem., Int. Ed.* **2002**, *41*, 2408.

(7) Bronstein, H.; et al. *J. Am. Chem. Soc.* **2011**, *133*, 3272.

(8) Ito, Y.; Virkar, A. A.; Mannsfeld, S.; Oh, J. H.; Toney, M.; Locklin, J.; Bao, Z. *J. Am. Chem. Soc.* **2009**, *131*, 9396.

(9) (a) Li, Y.; Sonar, P.; Singh, S. P.; Soh, M. S.; van Meurs, M.; Tan, J. *J. Am. Chem. Soc.* **2011**, *133*, 2198. (b) Zhang, M.; Tsao, H. N.; Pisula, W.; Yang, C.; Mishra, A. K.; Müllen, K. *J. Am. Chem. Soc.* **2007**, *129*, 3472.

(10) Rivnay, J.; Noriega, R.; Northrup, J. E.; Kline, R. J.; Toney, M. F.; Salleo, A. *Phys. Rev. B* **2011**, *83*, 121306(R).

(11) Brédas, J.-L.; Beljonne, D.; Coropceanu, V.; Cornil, J. *Chem. Rev.* **2004**, *104*, 4971.

(12) (a) Rivnay, J.; Steyrleuthner, R.; Jimison, L. H.; Casadei, A.; Chen, Z.; Toney, M. F.; Facchetti, A.; Neher, D.; Salleo, A. *Macromolecules* **2011**, *44*, 5246. (b) Zhang, X.; Richter, L. J.; DeLongchamp, D. M.; Kline, R. J.; Hammond, M. R.; McCulloch, I.; Heeney, M.; Ashraf, R. S.; Smith, J. N.; Anthopoulos, T. D.; Schroeder, B.; Geerts, Y. H.; Fischer, D. A.; Toney, M. F. *J. Am. Chem. Soc.* **2011**, *133*, 15073.

■ NOTE ADDED AFTER ASAP PUBLICATION

Due to a production error, GPC was incorrectly defined as "gas-phase chromatography" rather than "gel permeation chromatography" in the text in the version published ASAP November 28, 2011. The corrected version was reposted November 30, 2011.